Theoretical Study on Photophysical Properties of Bis-Dipolar Diphenylamino-Endcapped Oligoarylfluorenes as Light-Emitting Materials

Yan-Ling Liu,[†,‡] Ji-Kang Feng,*[,†,‡] and Ai-Min Ren[†]

State Key Laboratory of Theoretical and Computational Chemistry, Institute of Theoretical Chemistry, and The College of Chemistry, Jilin University, Changchun 130023 China

Received: October 29, 2007; In Final Form: January 6, 2008

Bis-dipolar emissive oligoarylfluorenes, OF(2)Ar-NPhs(2), bearing an electron affinitive core, 9,9-dibutylfluorene, as conjugated bridges and diphenylamino as endcaps, show great potential for application in organic light-emitting diodes. The various electron affinitive central aryl cores that include thiophene *S,S′*-dioxide, dibenzothiophene *S,S′*-dioxide, 2,1,3-benzothiadiazole, 4,7-dithien-2-yl-2,1,3-benzothiazole, dibenzothiophene, and dibenzofuran produce a remarkable influence on their optical and electronic properties. In this contribution, we apply quantum-chemical techniques to investigate a series of bis-dipolar diphenylamino-endcapped oligoaryfluorenes, OF(2)Ar-NPhs(2). The geometric and electronic structures in the ground state are studied using density functional theory (DFT) and the ab initio HF, whereas the lowest singlet excited states are optimized with ab initio CIS. The maximal absorption and emission wavelengths are investigated by employing time-dependent density functional theory (TDDFT). As a result, HOMOs, LUMOs, energy gaps, ionization potentials, electron affinities, and reorganization energies are affected by varying the electron affinitive cores in OF(2)Ar-NPhs(2). The absorption and emission spectra of this series of bis-dipolar oligoarylfluorenes also exhibit red shifts to some extent due to the electron-withdrawing property and the conjugated length of the electron affinitive cores. Remarkably, their calculated emission spectra can cover the full UV−vis spectrum (from 412 to 732 nm). Also, the Stokes shifes are unexpectedly large, ranging from 34 to 234 nm, resulting from a more planar conformation of the excited state between the two adjacent units in the oligoarylfluorenes. All the calculated results show that the oligoarylfluorenes can be used as hole and electron transport/injection materials in organic light-emitting diodes.

1. Introduction

In a recent publication we reported on the structural, optical, and electronic properties of a series of D−π−A−π−D type bis-dipolar emissive oligoarylfluorenes, OF(2)Ar-NPhs.[1] These phenyl-based π-conjugated oligomers have received recent attention for potential applications in organic light-emitting diodes (OLEDs) that take advantage of their excellent chemical, thermal, and photochemical stabilities as well as ease of structural tuning to adjust the electronic and morphological properties.[2−9] Experimentally, these bis-dipolar emissive oligoarylfluorenes have been synthesized and purified, and depending on the electronic nature of the central aryl moiety, their emissive colors can span almost the full UV−vis spectrum.[2] Because of the low first ionization potentials, good luminescence properties, high thermal stabilities, and good amorphous morphological stabilities of OF(2)Ar-NPhs, in this work we extend our earlier theoretical study to a computational investigation of another series of bis-dipolar diphenylamino-endcapped oligoaryfluorenes, defined as OF(2)Ar-NPhs(2) (shown in Figure 1) due to the different electron affinitive cores in the oligoarylfluorenes compared with OF(2)Ar-NPhs.[1] Density functional theory (DFT), single excitation configuration interaction (CIS), and time-dependent density functional theory (TDDFT) calculations have been carried out for these oligoaryfluorenes. Highest occupied molecular orbitals (HOMOs), lowest unoccupied molecular orbitals (LUMOs), energy gaps, ionization potentials, electron affinities, reorganization energies, and molecular modeling of the oligoarylfluorenes indicate that OF(2)Ar-NPhs-(2) can be used as hole transport/injection materials and are also good electron-accepting materials. Specifically, electronic absorption and emission spectra have been calculated for these bis-dipolar molecules. It has been shown that these oli-

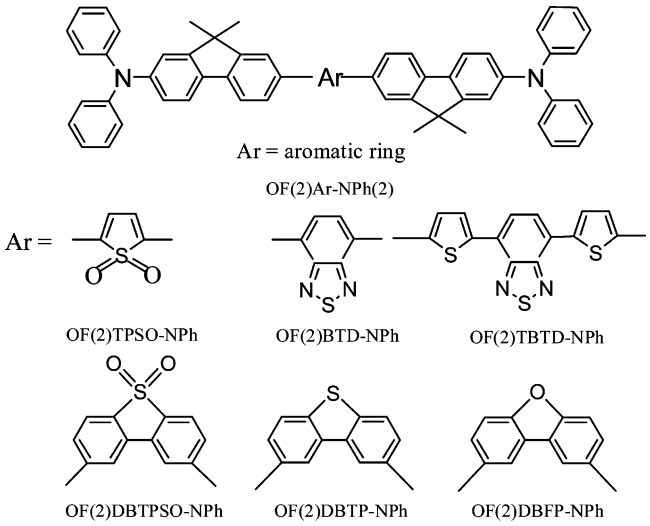

Figure 1. Sketch map of the structures of OF(2)Ar-NPhs(2).

* Corresponding author. Phone: +86-431-88499856. Fax: +86-431-88498026. E-mail: JiKangf@yahoo.com.

† State Key Laboratory of Theoretical and Computational Chemistry, Institute of Theoretical Chemistry.

‡ The College of Chemistry.

10.1021/jp7104067 CCC: $40.75
Published on Web 02/29/2008

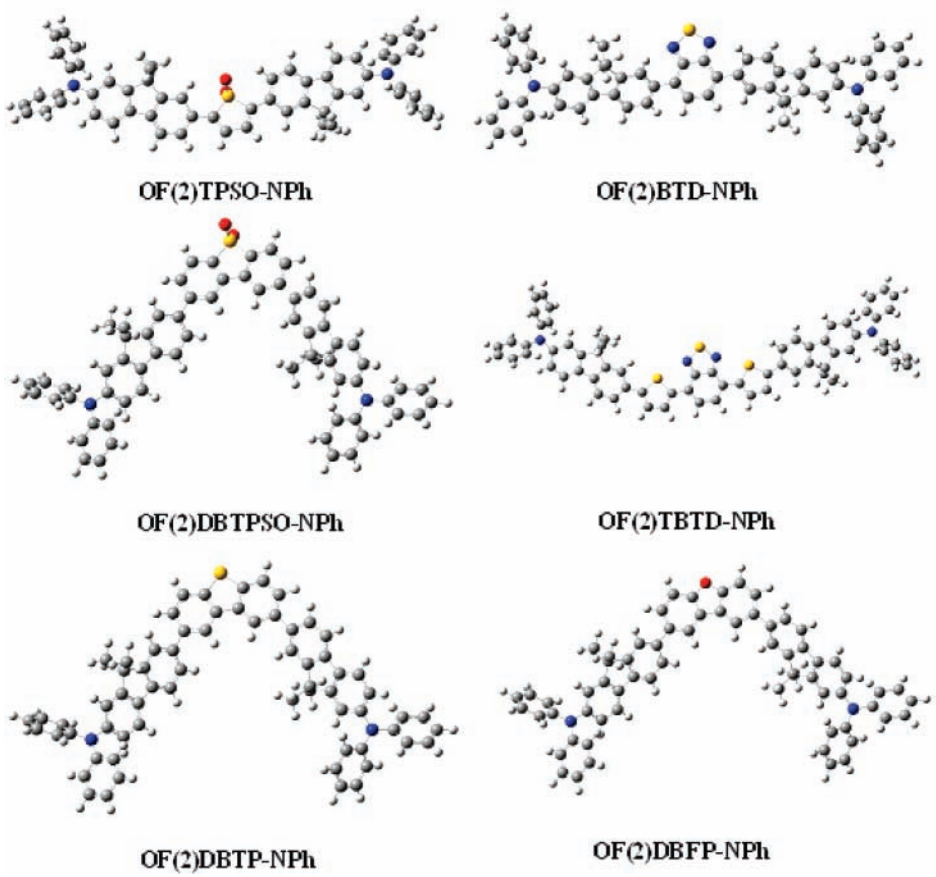

Figure 2. Optimized structures of OF(2)Ar-NPhs(2) by DFT//B3LYP/6-31G(d).

TABLE 1: Important Inter-Ring Distances and Dihedral Angles of OF(2)Ar-NPhs(2) in the Ground State with DFT//B3LYP/6-31G(d)[a]

	inter-ring distances (Å)				dihedral angles (deg)				
molecule	D−π	π−A	A−π	π−D	D−π	π−A	A−π	π−D	dipole moment (D)
OF(2)TPSO-NPh	1.418	1.455	1.455	1.418	38.5	21.8	23.9	39.6	3.07
OF(2)DBTPSO-NPh	1.418	1.484	1.484	1.418	38.6	39.0	38.8	39.3	8.32
OF(2)BTD-NPh	1.420	1.479	1.479	1.420	41.4	34.5	36.9	41.0	1.49
OF(2)TBTD-NPh	1.419	1.464	1.464	1.420	40.2	25.5	23.5	40.8	1.47
OF(2)DBTP-NPh	1.421	1.485	1.484	1.420	40.9	38.8	38.4	41.0	1.72
OF(2)DBFP-NPh	1.421	1.485	1.485	1.421	41.9	38.6	38.7	41.3	1.22

[a] D, diphenylamino; π, dimethylfluorene; A, electron affinitive core.

goarylfluorenes endcapped with diphenylamino moieties exhibit improved OLED device performance.

2. Computational Details

We have chosen the SGI origin 2000 server with the Gaussian 03 program package[10] to perform the geometry optimizations, spectra analysis, and excited state evaluations. The ground state geometries of OF(2)Ar-NPhs(2), as well as their cationic and anionic molecules, were fully optimized by DFT using the B3LYP hybrid functional combined with the 6-31G(d) basis set. There is no symmetric constraint on the geometric optimization. The lowest singlet excited state structures were calculated with ab initio CIS/6-31G(d) based on the optimized geometries obtained from HF/6-31G(d). Following each optimized structure, the electronic absorption and emission spectra were systematically investigated by the TDDFT method. The various properties of OF(2)Ar-NPhs(2), such as HOMOs, LUMOs, energy gaps, ionization potentials, electron affinities, and reorganization energies are obtained from the computed results and are compared to the available experimental data.

3. Results and Discussion

3.1. Molecular Structures. Figure 2 shows the optimized structures of bis-dipolar diphenylamino-endcapped oligoarylfluorenes, OF(2)Ar-NPhs(2), and a summary of the important inter-ring bond lengths, dihedral angles, and dipole moments is given in Table 1. Like earlier investigations, in contrast to the oligoarylfluorenes in the literature,[2] OF(2)Ar-NPhs(2) in this paper substitute butyl with methyl in fluorene rings for the sake of reducing the time of calculation.

In the ground state, the DFT calculated results show that the structures of dibutylfluorenes (D) and diphenylaminos (π) in OF(2)Ar-NPhs(2) do not suffer appreciable variations with the different electron affinitive cores (A). The main structural changes occur between the two adjacent units, especially π and A. In OF(2)TPSO-NPh and OF(2)DBTPSO-NPh, due to relieving unfavorable steric interactions between fluorene rings and thiophene *S*,*S*′-dioxide or dibenzothiophene *S*,*S*′-dioxide, the π−A bond lengths and dihedral angles increase from 1.455 to 1.484 Å and from 21.8° to 39.0°, respectively. In fact, the structural variations in OF(2)TBTD-NPh and OF(2)BTD-NPh

TABLE 2: Important Inter-Ring Distances and Dihedral Angles of OF(2)Ar-NPhs(2) in the Ground State with HF/6-31G(d)[a]

	inter-ring distances (Å)				dihedral angles (deg)				
molecule	D−π	π−A	A−π	π−D	D−π	π−A	A−π	π−D	dipole moment (D)
OF(2)TPSO-NPh	1.414	1.474	1.474	1.414	44.1	36.2	38.0	44.2	4.19
OF(2)DBTPSO-NPh	1.414	1.490	1.490	1.414	44.5	46.0	46.0	44.3	8.25
OF(2)BTD-NPh	1.416	1.487	1.487	1.416	46.2	44.0	45.7	46.1	1.91
OF(2)TBTD-NPh	1.416	1.478	1.478	1.416	45.9	38.6	38.2	45.8	2.47
OF(2)DBTP-NPh	1.416	1.491	1.491	1.416	46.4	45.9	46.0	46.4	1.77
OF(2)DBFP-NPh	1.416	1.496	1.496	1.416	46.7	46.3	46.5	46.6	1.23

[a] D, diphenylamino; π, dimethylfluorene; A, electron affinitive core.

TABLE 3: Important Inter-Ring Distances and Dihedral Angles of OF(2)Ar-NPhs(2) in the Excited State with CIS/6-31G(d)[a]

	inter-ring distances (Å)				dihedral angles (deg)				
molecule	D−π	π−A	A−π	π−D	D−π	π−A	A−π	π−D	dipole moment (D)
OF(2)TPSO-NPh	1.408	1.422	1.422	1.408	39.3	0.2	0.2	38.5	3.98
OF(2)DBTPSO-NPh	1.389	1.441	1.490	1.415	45.4	18.4	34.5	45.3	9.61
OF(2)BTD-NPh	1.409	1.443	1.443	1.409	40.0	19.7	19.8	39.8	1.80
OF(2)TBTD-NPh	1.414	1.460	1.460	1.413	43.8	21.2	19.9	43.6	2.21
OF(2)DBTP-NPh	1.394	1.447	1.490	1.416	37.6	19.8	45.3	46.5	2.58
OF(2)DBFP-NPh	1.393	1.454	1.491	1.416	37.9	23.0	45.9	46.7	1.90

[a] D, diphenylamino; π, dimethylfluorene; A, electron affinitive core.

are like those in OF(2)TPSO-NPh and OF(2)DBTPSO-NPh. Interestingly, due to their sharing the same group in the table of elements, the presence of the atoms oxygen and sulfur leads to only small changes in the inter-ring distances and dihedral angles for OF(2)DBTP-NPh and OF(2)DBFP-NPh. As a result, the two compounds have the very similar conformations, indicating their similar optical and electronic properties. It can be noted that OF(2)DBTPSO-NPh, OF(2)DBTP-NPh, and OF(2)DBFP-NPh exhibit high-nonplanar conformation and their structures tend to be bending in a butterfly shape owing to the strong steric hindrance influence of the electron affinitive cores. Compared with the DFT calculated results, the Hartree−Fock (HF) approach overestimates the dihedral angles between the two adjacent units in the oligoarylfluorenes, D and π, and π and A.

Electronic excitation leads to the large varieties of the oligoarylfluorene structures as shown in Tables 2 and 3. Both the inter-ring bond lengths and dihedral angles are shortened, especially for π and A. For example, the π−A bond lengths and dihedral angles in OF(2)BTD-NPh and OF(2)TBTD-NPh reduce from 1.487 to 1.443 Å, 44.0° to 19.7°, and from 1.478 to 1.460 Å, 38.6° to 21.2°, respectively. Also, the OF(2)DBTP-NPh excited structure is similar to that of OF(2)DBFP-NPh. This implies that the singlet excited structures between the two adjacent units in the oligoarylfluorenes should be more planar than their ground structures. Particularly, in OF(2)TPSO-NPh, the inter-ring dihedral angles between π and A are nearly 0°, which indicates that the diphenylamino and thiophene *S*,*S*′-dioxide in OF(2)TPSO-NPh may be coplanar in the excited state.

The dipole moment values of OF(2)Ar-NPhs(2) are collected in the last columns of Tables 1−3. The HF data are higher than those calculated by DFT in the ground state except OF(2)-DBTPSO-NPh. Notably, the dipole moments of OF(2)DBTPSO-NPh (DFT, 8.32 D; HF, 8.25 D; CIS, 9.61 D) are the largest. This may be attributed to its high-nonplanar conformation in comparison to OF(2)TPSO-NPh, OF(2)BTD-NPh, and OF(2)-TBTD-NPh. On the other hand, compared with OF(2)DBTP-NPh and OF(2)DBFP-NPh, more heteroatoms is the reason for the largest dipole moment of OF(2)DBTPSO-NPh.

3.2. Frontier Molecular Orbitals. It is well-known that the HOMOs, LUMOs, and energy gaps are weightily related to the optical and electronic properties. To gain insight into the influence of the various electron affinitive cores in OF(2)Ar-NPhs(2), sketches of the HOMOs and LUMOs of the oligoarylfluorenes by DFT//B3LYP/6-31G(d) are plotted in Figure 3. The calculated HOMO and LUMO energies and energy gaps are listed in Table 4, together with the experimental results. In addition, the total density of states (DOS) of OF(2)Ar-NPhs(2) has been compared in Figure 4 to more easily and vividly observe the varieties of the HOMOs, LUMOs, and energy gaps.

Here, our calculated energy gap in theory is the orbital energy difference between HOMO and LUMO, termed the HOMO−LUMO gap (Δ_{H-L}).[11−13] Experimentally, it is most obtained from the absorption spectra, which is the lowest transition (or excitation) energy from the ground state to the first dipole-allowed excited state, termed the optical band gap (E_g). In fact, the optical band gap is not the orbital energy difference between HOMO and LUMO, but the energy difference between the S_0 and S_1 states. Only when the excitation to the S_1 state corresponds almost exclusively to the promotion of the electron from the HOMO to the LUMO may the values of the optical band gap and the HOMO−LUMO gap be approximately equal. In this paper, we also theoretically calculated the optical band gaps of OF(2)Ar-NPhs(2) at the TDDFT level. As mentioned above, these optical band gaps are obtained from the absorption spectra.

The frontier orbitals all show π characteristics as visualized in Figure 3. For OF(2)TPSO-NPh, OF(2)BTD-NPh, and OF(2)TBTD-NPh, the HOMO orbitals are spread over the whole conjugated molecules, but the LUMO orbitals are mainly localized on the electron affinitive cores. However, for OF(2)-DBTPSO-NPh, OF(2)DBTP-NPh, and OF(2)DBFP-NPh, the HOMO orbitals are distributed on the dibutylfluorenes and diphenylaminos, but the LUMO orbitals are centralized on the diphenylaminos and the electron affinitive cores. In general, the HOMO orbitals possess bonding character and the LUMO orbitals hold antibonding character, although the HOMO orbitals show an antibonding interaction between the two adjacent subunits, D and π, and π and A, and the LUMO orbitals nicely show the bonding interaction in these regions, which is also reflected in the shorting of the corresponding inter-ring bond lengths in the excited states. In fact, because the lowest singlet excited state corresponds almost exclusively to the excitation

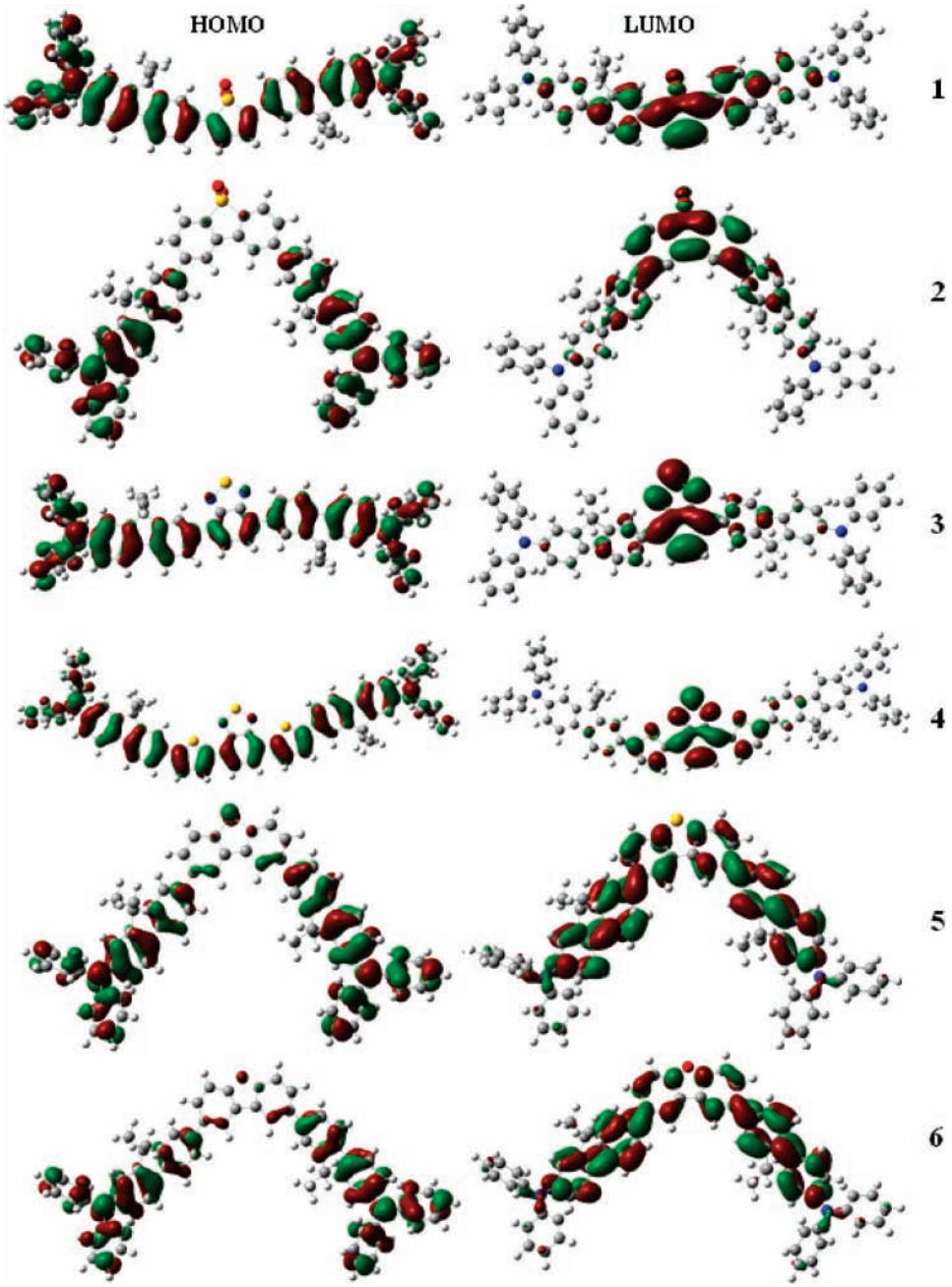

Figure 3. Frontier molecular orbitals of OF(2)Ar-NPhs(2) (1, OF(2)TPSO-NPh; 2, OF(2)DBTPSO-NPh; 3, OF(2)BTD-NPh; 4, OF(2)TBTD-NPh; 5, OF(2)DBTP-NPh; 6, OF(2)DBFP-NPh) by DFT//B3LYP/6-31G(d).

TABLE 4: Comparison between the Experimental and Calculated HOMO, LUMO Energies, HOMO−LUMO Gaps by DFT, and the Lowest Excitation Energies by TDDFT in eV for OF(2)Ar-NPhs(2)[a]

molecule	$-\epsilon_{HOMO}$	exptl[b]	$-\epsilon_{LUMO}$	exptl[c]	Δ_{H-L}	E_g(TD)	exptl[d]
OF(2)TPSO-NPh	4.80	5.22	2.33	3.12	2.47	2.16	2.10
OF(2)DBTPSO-NPh	4.97	5.22	1.82	2.43	3.15	2.85	2.79
OF(2)BTD-NPh	4.77	5.14	2.32	2.72	3.45	2.12	2.42
OF(2)TBTD-NPh	4.67	5.12	2.58	3.06	2.09	1.81	2.06
OF(2)DBTP-NPh	4.82	5.18	1.12	2.12	3.70	3.25	3.06
OF(2)DBFP-NPh	4.81		1.09		3.72	3.28	

[a] The HOMO and LUMO energies are given in negative and the experimental data (exptl) are taken from ref 2. [b] $E_{1/2}$ versus Fc^t/Fc estimated by CV method using a platinum disk electrode as a working electrode, platinum wire as a counter electrode, and SCE as a reference electrode with an agar salt bridge connecting to the oligomer solution. Ferrocene was used as an external standard, $E_{1/2}(Fc/Fc^t)$ 0.45 V versus SCE. [c] LUMO = HOMO − energy gap. [d] Energy gap was estimated from the absorption edge.

from the HOMO to the LUMO in all the considered oligoarylfluorenes, we can explore the differences in the bond lengths between the ground (S_0) and lowest singlet excited state (S_1) from MO nodal patterns. For example, as shown in Figure 3, Table 2, and Table 3, the HOMO orbitals of OF(2)Ar-NPhs-(2) have nodes between the two adjacent subunits, D and π, and π and A, whereas the LUMO orbitals are bonding in these regions. Therefore, we can expect the contraction of these inter-

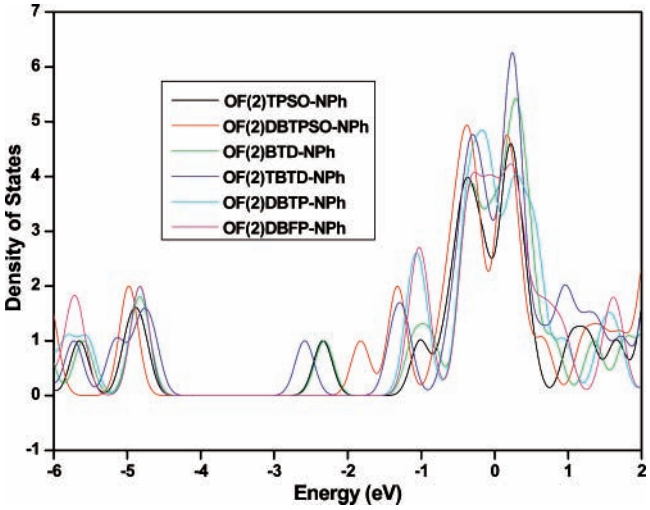

Figure 4. Total of density of states of OF(2)Ar-NPhs(2).

ring bond lengths; actually, the data in Table 3 confirm that these inter-ring bond lengths are considerably shorter in the excited state as discussed earlier.

From Figure 4 and Table 4, it can be seen that, although there are some discrepancies between the calculated data and experimental results, the variation trends of the HOMO and LUMO energies and energy gaps are similar. The presence of the various electron affinitive cores leads to only small changes in the HOMO energies of OF(2)Ar-NPhs(2), which are similar to those of OF(2)Ar-NPhs.[1] This suggests that cooperation with the different central aromatic rings does not weaken their hole-creating ability. Also, such a high HOMO energy level greatly reduces the energy barrier for the hole injection. Like OF(2)-Ar-NPhs studied earlier, OF(2)Ar-NPhs(2) also can be used as a good hole transport/injection material. Unlike the HOMO energies, the LUMO energies of OF(2)Ar-NPhs(2) vary much with the different electron affinitive cores. The LUMO energies of OF(2)TPSO-NPh, OF(2)BTD-NPh, and OF(2)TBTD-NPh are all much lower than those of OF(2)DBTPSO-NPh, OF(2)DBTP-NPh, OF(2)DBFP-NPh, and OF(2)Ar-NPhs,[1] which are −2.33, −2.32, and −2.58 eV, respectively, indicating the improvement of their electron-accepting ability. It is obvious that OF(2)TPSO-NPh, OF(2)BTD-NPh, and OF(2)TBTD-NPh are the better electron-accepting materials.

As expected, for OF(2)TPSO-NPh, OF(2)BTD-NPh, and OF-(2)TBTD-NPh, the energy gaps, whether Δ_{H-L}'s or E_g's, are much narrower than those of OF(2)DBTPSO-NPh, OF(2)DBTP-NPh, and OF(2)DBFP-NPh, due to the small changes in the HOMO energies but large varieties in the LUMO energies by the various electron affinitive cores. This may predict that the chain-shaped molecules have the larger absorption and emission wavelengths than the butterfly-shaped molecules. Comparing OF(2)TPSO-NPh and OF(2)DBTPSO-NPh, OF(2)BTD-NPh, and OF(2)TBTD-NPh, respectively, we can find that the HOMOs, LUMOs, and energy gaps, including Δ_{H-L} and E_g, are affected by the electron-withdrawing property and the conjugated length of the electron affinitive cores. The stronger the electron-withdrawing strength or the longer the conjugated length, the higher is the HOMO energies, the lower is the LUMO energies, and the narrower is the energy gap. Additionally, we can forecast that the absorption and emission spectra of OF(2)DBTP-NPh and OF(2)DBFP-NPh may be alike as a result of their similar HOMO and LUMO energies and energy gaps. These results indicate that the HOMOs, LUMOs, and energy gaps of OF(2)Ar-NPhs(2) are affected by the use of various electron affinitive cores.

3.3. Ionization Potentials and Electron Affinities. As mentioned in the Introduction, these oligoarylfluorenes, OF(2)-Ar-NPhs(2), can act as hole and electron transport/injection materials for OLEDs. Also, the device performance of OLEDs depends on efficient charge (hole and electron) injection, transfer, and balance as well as the exciton confinement in a device. In this paper, we calculated the ionization potentials (IPs), electron affinities (EAs), and reorganization energies (λ's) of OF(2)Ar-NPhs(2) by the DFT method and list them in Table 5. The ionization potentials and electron affinities both include the vertical excitations (at the geometry of the neutral molecule), adiabatic excitations (optimized structure for both the neutral and charged molecules), and extraction potentials (HEP and EEP for the hole and electron, respectively) that refer to the geometry of the ions. Here, the ionization potentials and electron affinities are used to estimate the energy barrier for the injection of holes and electrons into the oligoarylfluorenes, respectively, and the reorganization energies are used to value the charge transfer (or transport) rate and balance of OF(2)Ar-NPhs(2).

Obviously, the varied trends of the ionization potentials and electron affinities of OF(2)Ar-NPhs(2) are similar to those of the negative of the HOMO and LUMO energies. The ionization potentials of OF(2)Ar-NPhs(2) change little with the various electron affinitive cores, suggesting that the energy barriers required to create holes of these oligoarylfluorenes are alike. In contrast to the ionization potentials, the different electron affinitive cores have a great influence on the electron affinities of OF(2)Ar-NPhs(2). OF(2)TPSO-NPh, OF(2)BTD-NPh, and OF(2)TBTD-NPh have higher electron affinities than OF(2)-DBTPSO-NPh, OF(2)DBTP-NPh, and OF(2)DBFP-NPh. For example, the electron affinity of OF(2)TBTD-NPh is 1.63 eV, but that of OF(2)DBFP-NPh is 0.37 eV. For OF(2)DBTPSO-NPh and OF(2)TPSO-NPh, OF(2)BTD-NPh, and OF(2)TBTD-NPh, with the electron-withdrawing strength or the conjugated length of the electron affinitive cores, the ionization potentials decrease and the electron affinities increase. The ionization potentials and electron affinities of OF(2)DBTP-NPh and OF-(2)DBFP-NPh are very similar. All these results are in accord with the analysis from the HOMO and LUMO energies and suggest that these oligoarylfluorenes OF(2)Ar-NPhs(2) show great potential as hole and electron injection materials for OLEDs.

Generally, organic π-conjugated materials are assumed to transport charge at room temperature via a thermally activated hopping-type mechanism[14−17] and the vast majority of these organic conductive materials are p-type, so the hole-transfer process between adjacent spatially separated segments can be summarized as follows:

$$M^+ + M \rightarrow M + M^+$$

where M represents the neutral species undergoing charge transfer, and the M^+ species contains the hole. If the temperature is sufficiently high to treat vibrational modes classically, then the standard Marcus/Hush model yields the following expression for the hole (or electron) charge transfer rate,[18−21] assuming that hole traps are degenerate:

$$\kappa_{hole} = \left(\frac{\pi}{\lambda k_B T}\right)^{1/2} \frac{V^2}{\hbar} \exp\left(-\frac{\lambda}{4k_B T}\right) \quad (1)$$

where T is the temperature, k_B is the Boltzmann constant, λ is the reorganization energy due to geometric relaxation accompanying charge transfer, and V is the electronic coupling matrix element between the two species, which dictated largely

TABLE 5: Ionization Potentials, Electron Affinities, Extraction Potentials, and Reorganization Energies for Each Molecule (in eV) by DFT[a]

molecule	IP(v)	IP(a)	HEP	EA(v)	EA(a)	EEP	λ_{hole}	$\lambda_{electron}$
OF(2)TPSO-NPh	5.61	5.52	5.43	1.23	1.49	1.71	0.18	0.48
OF(2)DBTPSO-NPh	5.76	5.72	5.68	0.81	0.98	1.13	0.08	0.32
OF(2)BTD-NPh	5.55	5.48	5.40	1.08	1.29	1.50	0.15	0.42
OF(2)TBTD-NPh	5.38	5.29	5.18	1.47	1.63	1.77	0.20	0.30
OF(2)DBTP-NPh	5.59	5.54	5.49	0.27	0.41	0.55	0.10	0.28
OF(2)DBFP-NPh	5.58	5.53	5.48	0.25	0.37	0.50	0.10	0.25

[a] The suffixes (v) and (a) indicate vertical and adiabatic values, respectively.

TABLE 6: Electronic Transition Data Obtained by TDDFT for OF(2)Ar-NPhs(2) at the DFT//B3LYP/6-31G(d) Optimized Geometry[a]

		TDDFT//B3LYP/6-31G(d)				exptl[a]	
molecule	electronic transition	λ_{abs} (nm)	f	main configurations		λ_{abs} (nm)	f
OF(2)TPSO-NPh	$S_0 \rightarrow S_1$	574	1.33	HOMO $\rightarrow$ LUMO	0.67	503	2.85
OF(2)DBTPSO-NPh	$S_0 \rightarrow S_3$	378	0.50	HOMO$-$1 $\rightarrow$ LUMO$+$1	0.48	386	6.21
				HOMO $\rightarrow$ LUMO	0.11		
				HOMO $\rightarrow$ LUMO$+$1	0.14		
				HOMO $\rightarrow$ LUMO$+$2	0.44		
OF(2)BTD-NPh	$S_0 \rightarrow S_3$	427	0.21	HOMO$-$2 $\rightarrow$ LUMO	0.67	450	6.70
OF(2)TBTD-NPh	$S_0 \rightarrow S_3$	534	0.14	HOMO$-$2 $\rightarrow$ LUMO	0.67	526	7.70
OF(2)DBTP-NPh	$S_0 \rightarrow S_1$	382	1.08	HOMO$-$1 $\rightarrow$ LUMO$+$1	0.37	368	8.72
				HOMO $\rightarrow$ LUMO	0.56		
OF(2)DBFP-NPh	$S_0 \rightarrow S_1$	378	1.30	HOMO$-$1 $\rightarrow$ LUMO$+$1	-0.36		
				HOMO$-$1 $\rightarrow$ LUMO$+$2	-0.11		
				HOMO $\rightarrow$ LUMO	0.56		

[a] Measured in $CHCl_3$ (ref 2).

TABLE 7: Emission Data Obtained by TDDFT for OF(2)Ar-NPhs(2) at the CIS/6-31G(d) Optimized Geometry[a]

		TDDFT//B3LYP/6-31G(d)					exptl[a]	
molecule	electronic transition	λ_{em}(nm)	f	main configurations		τ (ns)	λ_{em} (nm)	τ (ns)
OF(2)TPSO-NPh	$S_1 \rightarrow S_0$	687	1.60	HOMO $\rightarrow$ LUMO	0.63	4.42	644	2.10
OF(2)DBTPSO-NPh	$S_1 \rightarrow S_0$	460	1.03	HOMO $\rightarrow$ LUMO	0.66	3.06	530	1.29
OF(2)BTD-NPh	$S_1 \rightarrow S_0$	661	1.02	HOMO $\rightarrow$ LUMO	0.66	6.42	608	1.63
OF(2)TBTD-NPh	$S_1 \rightarrow S_0$	732	1.29	HOMO $\rightarrow$ LUMO	0.64	6.21	656	1.73
OF(2)DBTP-NPh	$S_1 \rightarrow S_0$	420	1.39	HOMO $\rightarrow$ LUMO	0.65	1.90	412	1.50
OF(2)DBFP-NPh	$S_1 \rightarrow S_0$	412	1.45	HOMO $\rightarrow$ LUMO	0.65	1.75		

[a] Measured in $CHCl_3$ (ref 2).

in transfer processes is very important. It is clear that two key parameters are the reorganization energy and electronic coupling matrix element, which have a dominant impact on the charge-transfer rate, especially the former. In this paper, we mainly investigate the effect of the reorganization energy in the charge-transfer processes. Here, the reorganization energy is just the internal reorganization energy of the isolated active organic π-conjugated systems due to ignoring any environmental relaxation and changes. Hence, the reorganization energy for hole transfer in eq 1 can be defined as[17]

$$\lambda = \lambda_0 + \lambda_+ = (E^*_0 - E_0) + (E^*_+ - E_+) \qquad (2)$$

As illustrated in Figure 5, E_0 and E_+ represent the energies of the neutral and cation species in their lowest energy geometries, respectively, while E^*_0 and E^*_+ represent the energies of the neutral and cation species with the geometries of the cation and neutral species, respectively. This description holds as long as the potential energy surfaces are harmonic, and the λ_0 and λ_+ terms are close in energy. In fact, many factors, including heteroatom identity, heterocycle substituents, and conjugation length, are known to be important in dictating the reorganization energy. As shown in Table 5, the various electron affinitive cores produce a remarkable influence on the reorganization energy of OF(2)Ar-NPhs(2). With the increase in electron-withdrawing strength or the decrease in conjugated length of the electron affinitive cores, the reorganization energy increases, and this indicates that the charge-transfer rate decreases. Because the λ_{hole}'s are all smaller than the $\lambda_{electron}$'s, OF(2)Ar-NPhs(2) can be used as better hole transport materials in the organic light-emitting diodes. Moreover, we find that OF(2)TBTD-NPh has the best charge transfer (or transport) balance performance because the difference between the λ_{hole} and $\lambda_{electron}$ is the least, only 0.1 eV.

3.4. Absorption and Emission Spectra. TDDFT//B3LYP/6-31G(d) has been used to obtain the absorption and emission spectra of OF(2)Ar-NPhs(2). The transition energies, oscillator strengths, and main configurations for the most relevant singlet excited states in each molecule are listed in Tables 6 and 7, respectively. For the absorption spectra, the calculated data are in good agreement with the experimental values. All the electronic transitions are of $\pi \rightarrow \pi^*$ type, and the excitation to the S_1 state corresponds mainly to the electron promotion from the HOMO to the LUMO. Interestingly, the absorption peaks of OF(2)DBTPSO-NPh, OF(2)BTD-NPh, and OF(2)TBTD-NPh are assigned to the $S_0 \rightarrow S_3$ electronic transition. Also, the HOMO$-$2 to LUMO excitation plays a dominant role in OF(2)BTD-NPh and OF(2)TBTD-NPh, but HOMO$-$2 to LUMO excitation does not play a dominant role in OF(2)DBTPSO-NPh. For the emission spectra, the emission peaks of OF(2)-Ar-NPhs(2) are also assigned to $\pi \rightarrow \pi^*$ character, arising from the S_1, HOMO $\rightarrow$ LUMO transition.

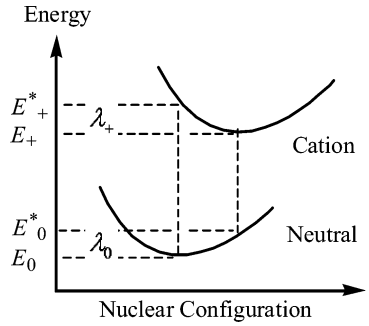

Figure 5. Internal reorganization energy for hole transfer.

As shown in Tables 6 and 7, the absorption and emission spectra of this series of bis-dipolar oligoarylfluorenes exhibit red shifts to some extent due to the electron-withdrawing property and the conjugated length of the electron affinitive cores (see the absorption and emission spectra of OF(2)TPSO-NPh and OF(2)DBTPSO-NPh, OF(2)BTD-NPh, and OF(2)-TBTD-NPh, respectively). Remarkably, their emission spectra calculated can cover the full UV−vis spectrum (from 412 to 732 nm). The Stokes shifes are unexpectedly large, ranging from 34 to 234 nm, which may result from a more planar conformation of the excited state between the two adjacent units in the oligoarylfluorenes, OF(2)Ar-NPhs(2). As expected, the main absorption and emission features in OF(2)DBTP-NPh and OF-(2)DBFP-NPh are very similar [the absorption spectra, 382 nm (OF(2)DBTP-NPh) and 378 nm (OF(2)DBFP-NPh); the emission spectra, 420 nm (OF(2)DBTP-NPh) and 412 nm (OF(2)-DBFP-NPh)]. These results confirm the prediction from the energy gap discussion above.

Moreover, we find in Table 6 that OF(2)TPSO-NPh, OF(2)-DBTP-NPh, and OF(2)DBFP-NPh have much larger oscillator strengths than OF(2)DBTPSO-NPh, OF(2)BTD-NPh, and OF-(2)TBTD-NPh. The oscillator strength[22] for an electronic transition is proportional to the transition moment. The transition moment reflects the transition probability from the ground state to the excited state. The transition moments of OF(2)Ar-NPhs-(2) are 5.01 (OF(2)TPSO-NPh), 2.47 (OF(2)DBTPSO-NPh), 1.71 (OF(2)BTD-NPh), 1.56 (OF(2)TBTD-NPh), 3.68 (OF(2)-DBTP-NPh), and 4.02 au (OF(2)DBFP-NPh), respectively. This means that the electronic transition probability of OF(2)TPSO-NPh, OF(2)DBTP-NPh, and OF(2)DBFP-NPh (the excitation to S_1 state) is higher than that of OF(2)DBTPSO-NPh, OF(2)-BTD-NPh, and OF(2)TBTD-NPh (the excitation to S_3 state). On the other hand, from Table 7, we also find that TDDFT calculations performed on the geometry optimized in the lowest excited state at the CIS level show that the $S_1 \rightarrow S_0$ transitions for OF(2)Ar-NPhs(2) have high oscillator strengths, which may be attributed to the influence of the molecular structure variety and the heteroatom in electronic excitation. This implies that these oligoarylfluorenes have large fluorescent intensity and they are useful as fluorescent OLED materials.

On the basis of the fluorescence energy and oscillator strength, the emission lifetimes (τ) were calculated for spontaneous emission by using the Einstein transition probabilities according to the formula (in au)[23,24]

$$\tau = \frac{c^3}{2(E_{\mathrm{Flu}})^2 f} \qquad (3)$$

where c is the velocity of light, E_{Flu} is the transition energy, and f is the oscillator strength. The calculated lifetime τ for the oligoarylfluorenes, OF(2)Ar-NPhs(2), are summarized in Table 7 and are good accord with the experimental data.[2] For example, the value of 1.90 ns of OF(2)DBTP-NPh shows agreement within realistic expectations since the experimentally observed lifetime is 1.50 ns. Also, the emission lifetimes of OF(2)TPSO-NPh, OF(2)BTD-NPh, and OF(2)TBTD-NPh are higher than those of OF(2)DBTPSO-NPh, OF(2)DBTP-NPh, and OF(2)-DBFP-NPh. In conclusion, these results further support that the optical and electronic properties of these oligoarylfluorenes can easily be modified or tuned by the use of various electron affinitive cores. Also, it is a key point toward the development of this sort of π-conjugated materials for OLEDs.

4. Conclusions

Due to great potential for application in organic light-emitting diodes, a series of bis-dipolar emissive oligoarylfluorenes, OF-(2)Ar-NPhs(2), has been systematically investigated in this work. Because of computational efficiency, DFT/B3LYP and ab initio HF methods have been used for the ground geometry optimizations and the lowest singlet excited states are optimized with ab initio CIS. Following each optimized structure, the electronic absorption and emission spectra are studied by the TDDFT method. The calculated results show that their optical and electronic properties, including HOMOs, LUMOs, energy gaps, ionization potentials, electron affinities, reorganization energies, and absorption and emission spectra, are affected by the electron affinitive cores of the oligoarylfluorenes, OF(2)Ar-NPhs(2). With the electron-withdrawing strength and the conjugated length of the electron affinitive cores, the HOMO energies, electron affinities, and reorganization energies increase, the LUMO energies and ionization potentials decrease, the energy gaps narrow, and the absorption and emission spectra exhibit red shifts to some extent. Importantly, the emission spectra of the oligoarylfluorenes can cover the full UV−vis spectrum (from 412 to 732 nm). The results presented show that varying the electron affinitive cores of bis-dipolar emissive oligoarylfluorenes is a highly promising approach to develop this series of materials for OLED applications.

Acknowledgment. This work is supported by the Major State Basic Research Development Program (2002CB 613406), the National Natural Science Foundation of China (Project No. 20673045), and the State Key Laboratory for Superamolecular Structure and Material of Jilin University.

References and Notes

(1) Liu, Y. L.; Feng, J. K.; Ren, A. M. *J. Phys. Org. Chem.* **2007**, *20*, 600−609.

(2) Li, Z. H.; Wong, M. S.; Fukutani, H.; Tao, Y. *Chem. Mater.* **2005**, *17*, 5032−5040.

(3) Li, Z. H.; Wong, M. S.; Tao, Y.; Lu, J. *Chem.—Eur. J.* **2005**, *11*, 3285−3293.

(4) Wong, M. S.; Li, Z. H.; Shek, M. F.; Chow, K. H.; Tao, Y.; D'Iorio, M. *J. Mater. Chem.* **2000**, *10*, 1805−1810.

(5) Wong, M. S.; Li, Z. H.; Tao, Y.; D'Iorio, M. *Chem. Mater.* **2003**, *15*, 1198−1203.

(6) Li, Z. H.; Wong, M. S.; Tao, Y.; D'Iorio, M. *J. Org. Chem.* **2004**, *69*, 921−927.

(7) Wong, M. S.; Li, Z. H. *Pure Appl. Chem.* **2004**, *76*, 1409−1419.

(8) Donat-Bouillud, A.; Lévesque, I.; Tao, Y.; D'Iorio, M.; Beaupré, S.; Blondin, P.; Ranger, M.; Bouchard, J.; Leclerc, M. *Chem. Mater.* **2000**, *12*, 1931−1936.

(9) Li, Z. H.; Wong, M. S. *Org. Lett.* **2006**, *8*, 1499−1502.

(10) Frisch, M. J.; Trucks, G. W.; Schlegel, H. B.; Scuseria, G. E.; Robb, M. A.; Cheeseman, J. R.; Montgomery, J. A., Jr.; Vreven, T.; Kudin, K. N.; Burant, J. C.; Millam, J. M.; Iyengar, S. S.; Tomasi, J.; Barone, V.; Mennucci, B.; Cossi, M.; Scalmani, G.; Rega, N.; Petersson, G. A.; Nakatsuji, H.; Hada, M.; Ehara, M.; Toyota, K.; Fukuda, R.; Hasegawa, J.; Ishida, M.; Nakajima, T.; Honda, Y.; Kitao, O.; Nakai, H.; Klene, M.; Li,

X.; Knox, J. E.; Hratchian, H. P.; Cross, J. B.; Adamo, C.; Jaramillo, J.; Gomperts, R.; Stratmann, R. E.; Yazyev, O.; Austin, A. J.; Cammi, R.; Pomelli, C.; Ochterski, J. W.; Ayala, P. Y.; Morokuma, K.; Voth, G. A.; Salvador, P.; Dannenberg, J. J.; Zakrzewski, V. G.; Dapprich, S.; Daniels, A. D.; Strain, M. C.; Farkas, O.; Malick, D. K.; Rabuck, A. D.; Raghavachari, K.; Foresman, J. B.; Ortiz, J. V.; Cui, Q.; Baboul, A. G.; Clifford, S.; Cioslowski, J.; Stefanov, B. B.; Liu, G.; Liashenko, A.; Piskorz, P.; Komaromi, I.; Martin, R. L.; Fox, D. J.; Keith, T.; Al-Laham, M. A.; Peng, C. Y.; Nanayakkara, A.; Challacombe, M.; Gill, P. M. W.; Johnson, B.; Chen, W.; Wong, M. W.; Gonzalez, C.; Pople, J. A. *Gaussian 03*, revision B. 04; Gaussian, Inc.: Pittsburgh, PA, 2003.

(11) Hay, P. J. *J. Phys. Chem. A* **2002**, *106*, 1634−1641.

(12) Curioni, A.; Andreoni, W.; Treusch, R.; Himpsel, F. J.; Haskal, E.; Seidler, P.; Heske, C.; Kakar, S.; van Buren, T.; Terminello, L. *J. Appl. Phys. Lett.* **1998**, *72*, 1575−1577.

(13) Hong, S. Y.; Kim, D. Y.; Kim, C. Y.; Hoffmann, R. *Macromolecules* **2001**, *34*, 6474−6481.

(14) Epstein, A. J.; Lee, W. P.; Prigodin, V. N. *Synth. Met.* **2001**, *117*, 9.

(15) Reedijk, J. A.; Martens, H. C. F.; van Bohemen, S. M. C.; Hilt, O.; Brom, H. B.; Michels, M. A. J. *Synth. Met.* **1999**, *101*, 475−476.

(16) Mott, N. F.; Davis, E. A. *Electronic Processes in Non-Crystalline Materials*, 2nd ed.; Oxford University Press: Oxford, 1979.

(17) Hutchison, G. R.; Ratner, M. A.; Marks, T. J. *J. Am. Chem. Soc.* **2005**, *127*, 2339−2350.

(18) Marcus, R. A. *Rev. Mod. Phys.* **1993**, *65*, 599−610.

(19) Marcus, R. A.; Eyring, H. *Annu. Rev. Phys. Chem.* **1964**, *15*, 155−196.

(20) Hush, N. S. *J. Chem. Phys.* **1958**, *28*, 962−972.

(21) Marcus, R. A. *J. Chem. Phys.* **1956**, *24*, 966−978.

(22) Peyerimhoff, S. D. In *The Encyclopedia of Computational Chemistry*; Schleyer, P. von R., Allinger, N. L., Clark, T., Gasteiger, J., Kollman, P. A., Schaefer, H. F., III, Schreiners, P. R. Eds.; Wiley: Chichester, U.K.; 1998; pp 2646−2664.

(23) Litani-Barzilai, I.; Bulatov, V.; Schechter, I. *Anal. Chim. Acta* **2004**, *501*, 151−156.

(24) Lukeš, V.; Aquino, A.; Lischka, H. *J. Phys. Chem. A* **2005**, *109*, 10232−10238.